JOURNAL OF MATERIALS SCIENCE 33 (1998) 2255–2268

The influence of the deformation temperature on the tensile properties of polyethylenes

A. J. PEACOCK*,‡, L. MANDELKERN*, R. G. ALAMO§
Department of Chemistry and Institute of Molecular Biophysics, Florida State University, Tallahassee, FL 32306, USA
E-mail: mandelk@sb.fsu.edu

J. G. FATOU†
Instituto de Ciencia y Tecnologia de Polimeros, Consejo Superior de Investigaciones Ciencias, Juan de la Cierva, 3 Madrid-28006, Spain

The force–elongation curves and key tensile parameters of a set of polyethylenes were studied over the temperature range from −100 °C to their respective melting temperatures, at a fixed strain rate. The polymers chosen possessed a diverse molecular architecture and constitution. They were crystallized in such a manner as to generate a wide range in crystallinity levels and supermolecular structures. Unique to this work are accompanying dilatometric studies. These enabled the changing level of crystallinity with temperature to be monitored. The force–elongation curves that were obtained varied in a systematic manner with the chain structure and deformation temperature. The yield stresses of all the polymers were very similar to one another in the region of the glass transition temperature. However, they diverged at elevated temperatures, depending on the chain structure, linear or branched, and the level of crystallinity. The change in the ultimate properties, the draw ratio, λ_B, after break and the true ultimate tensile strength, with deformation temperature could be correlated with the changing level of crystallinity. The temperature dependence of these properties are strongly dependent on molecular weight and, except for the very highest molecular weights, a maximum is observed. Possible mechanisms that govern the ultimate properties are presented and discussed. The temperature dependence of the yield stress could not be correlated with the dislocation theory that has been developed to describe yielding. © *1998 Chapman & Hall*

1. Introduction

The mechanical properties of semicrystalline polymers have received a great deal of attention and study because of their intrinsic scientific interest and practical importance. In addition to theoretical analyses there has been a great deal of interest in assessing the role of molecular constitution as well as the influence of the key structural variables that define the crystalline state. Molecular contributions includes the molecular weight, distribution, as well as the structural and chemical regularity of the chains. The independent structural variables include the level of crystallinity, the crystallite and interlamellar thicknesses and the supermolecular structure [1, 2]. Besides these variables, which are characteristic of the molecular system being studied, the roles of temperature and strain rate in the deformation process also need to be assessed. Because of the wide diversity of factors that have to be considered, the molecular and structural basis underlying the deformation process is not as well understood as would be desired. Recent force–elongation studies have been directed to assessing the role of molecular constitution and structural factors by isolating the different variables involved [3–7]. Several major features governing the deformation process emerged from these studies. In the main, the studies where the variables have been controlled have usually been limited to one deformation temperature and strain rate. To obtain a better understanding of the tensile behaviour of crystalline polymers these vistas need to be expanded.

In the present paper, attention is focused on the role of the deformation temperature on the tensile properties of a set of polyethylenes. The polymers studied

*To whom correspondence should be addressed.
‡ *Present address*: Baytown Polymers Center, Exxon Chemical Company, PO Box 5200, Baytown, TX 77522-5200, USA.
§ *Present address*: Department of Chemical Engineering, Florida Agricultural and Mechanical University–Florida State University, College of Engineering, 2525 Pottsdamer Street, Tallahassee, FL 32310-6046, USA.
† Deceased.

include linear and branched polyethylenes, so chosen to encompass a range in molar mass, polydispersity and molecular architectures. These samples were crystallized in such a manner so as to develop as wide a range as possible in crystallinity levels and supermolecular structures. The deformation temperatures varied from $-100\,^{\circ}C$ to close to the melting temperature of each polymer. Force–elongation curves were obtained over this temperature interval. The crystallinity levels of the samples were monitored from $-30\,^{\circ}C$ by volume dilatometric measurements. These corollary studies allowed an assessment to be made of the influence of the decreasing crystallinity on the key tensile parameters.

2. Experimental procedure

2.1. Materials

Five linear and three branched representative polyethylenes were chosen for study. Their molecular characteristics are listed in Table I. Because of the large amount of sample needed for each set of experiments, unfractionated, commercial materials were used. Consequently, the samples all had broad molecular weight distributions rather than the preferable narrow distributions [6]. Sample F was prepared by high-pressure free-radical polymerization. Consequently, together with the long-chain branches, short-chain branches consisting mainly of ethyl and butyl groups were also present. Sample G was also prepared by high-pressure free-radical polymerization. Therefore, in addition to the acetate branches it also contained olefinic branches similar to those found in polymer F. Sample H, with ethyl side groups is a conventional ethylene-1 alkene copolymer polymerized with a Ziegler–Natta-type catalyst. The value of the branch content given in Table I include all the branch types, as determined by conventional ^{13}C nuclear magnetic resonance [8, 9].

2.2. Methods

Samples were compression moulded in a hot press at temperatures about $25\,^{\circ}C$ above their peak melting temperature, as determined by differential scanning calorimetry (DSC). The samples were completely melted prior to the application of a load of about $550\ lbf\ in^{-2}$ to produce films approximately 0.25–0.50 mm thick. The molten films were allowed to equilibrate under pressure for 5 min prior to cooling. Samples to be slowly cooled were moulded between aluminium plates 6.4 mm thick lined with polytetrafluoroethylene sheets 1.6 mm thick. Prior to removal from the press, the resulting "sandwich" of metal and polymer was clamped together using spring clips. Upon removal from the press the sandwich was allowed to cool to room temperature on a wire cooling grid. Samples that were to be quenched were moulded between steel plates 0.8 mm thick lined with aluminium foil 0.1 mm thick. Prior to removal from the press, the sandwich was clamped together using vice grips. Upon removal from the press the sandwich was plunged directly into a slush bath of ice–water or dry ice–isopropanol at $0\,^{\circ}C$ or $-78\,^{\circ}C$, respectively. Samples that were to be isothermally crystallized were moulded in the same manner as quenched samples and then crystallized in oil baths set at the appropriate temperature, thermostated to $\pm 0.1\,^{\circ}C$.

The density of the moulded samples were determined to four significant figures by flotation in a density gradient column consisting of triethylene glycol and isopropanol. The degree of crystallinity on a density basis, $(1-\lambda)_d$, was calculated by the method of Chiang and Flory [10] using $1.000\ g\ cm^{-3}$ and $0.853\ g\ cm^{-3}$ for the densities of the crystalline and non-crystalline regions, respectively. The degree of crystallinity is calculated to $\pm 0.5\%$ by this method. This method was not applicable to sample G because the appropriate constant for the density of the non-crystalline region is unavailable.

Heats of fusion, Δh_f, and melting temperatures, T_M, were measured in a Perkin–Elmer DSC-2 calibrated with indium. Specimens of 3.0 ± 0.2 mg were sealed in aluminium pans and heated over the range 270–450 K at $10\,^{\circ}C\ min^{-1}$. The melting endotherm was defined by drawing a straight baseline from the onset of melting to its conclusion. The area of each endotherm was determined by planimetry. The degree of crystallinity determined by this method, $(1-\lambda)_{\Delta H}$, was calculated from Δh_f, assuming $69\ cal\ g^{-1}$ for completely crystalline polyethylene [11]. The error associated with this method is estimated to be $\pm 5\%$.

The degree of crystallinity of the samples was also determined by analysis of their Raman internal mode spectra, utilizing the method of Strobl and Hagedorn [12], as refined in this laboratory [13–15]. Three parameters describing the phase structure can be determined from the Raman internal modes. These are as follows: α_c, the fraction of chain units in the perfect crystal, i.e., the core crystallinity; α_a, the fraction of chain units in the liquid-like disordered region; α_b, the fraction of the system comprising the anisotropic interfacial region wherein the units are in a partially ordered state. The quantities α_c and α_a can be determined directly from the spectra. The interfacial fraction is defined as

$$\alpha_b = 1 - (\alpha_c + \alpha_a) \quad (1)$$

The supermolecular structures were characterized by small-angle light scattering using the photometer

TABLE I Characteristics of samples

Polymer Polyethylene type	$M_w \times 10^5$	M_w/M_n	Branch content[a]
A Linear	1.5	12.5	—
B Linear	5	5.5	—
C Linear	9.7	4.4	—
D Linear	20[b]	—	—
E Linear	80[b]	—	—
F Branched high-pressure	3.46	18.5	12.8
G Ethylene–vinyl acetate copolymer	—	—	21
H Ethylene–butene copolymer	1.4	7.1	17

[a] Branch points per 1000 carbon atoms.
[b] Viscosity average.

previously described [16]. The terminology that classifies the superstructures is the same as that used previously [16, 17]. Thus, a, b and c represent spherulitic morphology with decreasing structural order while h indicates the absence of a defined supermolecular structure.

The crystallization conditions and structural characteristics of the samples in the semicrystalline state are given in Table II.

The variation in the crystallinity level during fusion was followed over the range from $-30\,^{\circ}C$ to $150\,^{\circ}C$ by dilatometry. The dilatometers used were of the type initially described by Bekkedahl [18] that were modified for small quantities of sample [19–21]. The capillary of 0.5 mm diameter and the bulb, where the sample was confined, were set at a 90° angle. The dilatometers were filled with mercury under high vacuum. Approximately 500 mg of bubble-free sample was used. The dilatometers were further immersed in a thermostated oil bath whose temperature was controlled to $\pm 0.1\,^{\circ}C$. The temperature of the bath was increased in 2–3 °C increments. The dilatometers were held at each temperature until constant readings were attained. The calculations of the crystallinity levels were carried out as previously described [21]. The specific volume of the liquid (amorphous) polymer was calculated following the relation given by Chiang and Flory [10].

$$V_1 = 1.152 + 8.8 \times 10^{-4} T \ (T \text{ in } ^{\circ}C)$$

The non-linearity of the expansion coefficient, α_c, of the crystalline region was taken into account according to published data [21]. In the temperature interval between 0 and 50 °C, the α_c value reported by Quinn and Mandelkern [11] was used ($2.81 \times 10^{-4}\,K^{-1}$), and in the temperature interval 0–100 °C the value reported by Cole and Holmes [22] was taken ($2.95 \times 10^{-4}\,K^{-1}$). In the temperature interval between 100 and 150 °C the expansion coefficient was taken as $2.59 \times 10^{-4}\,K^{-1}$ [10]. Thus, the specific volume–temperature relations used are

$$V_c = 0.993 + 2.81 \times 10^{-4} T \text{ for } -50 \text{ to } 0\,^{\circ}C$$

$$V_c = 0.993 + 2.94 \times 10^{-4} T \text{ for } 0 \text{ to } 100\,^{\circ}C$$

$$V_c = 0.993 + 2.59 \times 10^{-4} T \text{ for } 100 \text{ to } 150\,^{\circ}C$$

Dumbbell-shaped specimens were used for the tensile experiments. They were cut from the compression moulded films with a die cutter and had a gauge length of 5 mm and a width of 2.56 mm. For a given sample and set of crystallization conditions, all the tensile test specimens were cut from a single film. Samples were drawn at a constant elongation rate of $25.4\ mm\ min^{-1}$. The deformations were carried out in two laboratories. C. S. Speed of Exxon Chemical Company at the Baytown Polymers Center carried out the deformation of samples at temperatures, T_d, from $-100\,^{\circ}C$ to room temperature, 22 °C. Deformation from 25 to 130 °C was carried out at the Instituto de Ciencia y Tecnologia de Polimeros, Madrid. Allowing for the slight discrepancy in temperatures, excellent agreement was achieved between the room-temperature results from the two laboratories. The two sets of data overlap in a continuous manner.

The yield stress, the draw ratio after break, λ_B, the ultimate tensile stress and the true ultimate tensile stress (TUTS), defined as the ultimate tensile force multiplied by λ_B divided by the original cross-sectional area, were determined as described previously [4]. Therefore, a homogeneous deformation is assumed in calculating TUTS. A minimum of six independent measurements were made for each set of conditions and the results averaged.

3. Results and discussion

3.1. Specimen characteristics

The values of some of the key structural parameters that describe and define the crystalline state are given in Table II, for each of the polymers studied, together with the corresponding crystallization conditions. It is important to note the wide range in crystallinity levels that is attained by varying the molecular weight and crystallization conditions. For the linear polyethylenes the level of crystallinity varies from about 46 to 80%, when calculated on the basis of the enthalpy of fusion. The crystallinity level is reduced to the 20–30% range for the structurally irregular branched chains. The observed melting temperatures, as determined by DSC at a heating rate of $10\ K\ min^{-1}$, vary from 102 to 140.5 °C. The latter, very high value was for

TABLE II Crystallization conditions and solid-state properties of the polyethylenes studied

Polymer	Crystallization conditions	$(1-\lambda)_d$ (%)	$(1-\lambda)_{\Delta II}$ (%)	α_c (%)	α_a (%)	α_b (%)	T_M (°C)	T_i (°C)	$T_{1/2}$ (°C)	Supermolecular structure
A	Slow cooled	81	67	75	17	8	136	35	130	h
A	128.5 °C, 17 days	90	82	87	10	3	140.5	70	135	h
B	Quenched, −78 °C	56	51	44	38	18	134.5	35	130	c
B	90 °C, 30 min	64	59	48	33	19	135.5	—	—	—
B	115 °C, 30 min	68	59	56	28	16	137	—	—	—
B	121 °C, 30 min	70	59	54	27	19	138	—	—	—
B	125 °C, 30 min	70	62	56	31	13	138.5	35	130	h
C	Slow cooled	64	53	51	35	14	135	—	—	c
D	Slow cooled	61	43	44	38	18	137.5	40	130	c
D	120 °C, 30 min	61	50	48	36	16	137	—	—	—
E	Slow cooled	59	46	42	39	19	133	40	130	h
F	Slow cooled	51	26	28	50	22	108.5	35	105	a
G	Quenched	—	27	30	50	20	120	20	95	h
H	Slow cooled	51	23	23	53	24	102	35	110	b

a specimen that was isothermally crystallized at a high temperature for an extremely long time. A range in the supermolecular structures has also been attained. In some cases, designated by the letter h, no supermolecular structures including spherulites, are observed. Before examining the temperature dependence of the tensile behaviour it is important that the fusion process be investigated. It can be expected that the changing level of crystallinity with temperature will influence the character of the force–elongation curves as well as the values of the key tensile parameters.

3.2. Melting behaviour

The crystallinity level, $1 - \lambda$, is plotted in Fig. 1a and b as a function of temperature for some of the linear and branched polymers, respectively, that were studied. The course of the fusion is of primary interest. The differences observed in the fusion process are those expected for the chain structures and crystallization conditions involved. For example, the fusion of the two structurally irregular chains (Fig. 1b) is broader and more diffuse than the linear polymers. For a given molecular weight, the melting of the linear polymer is

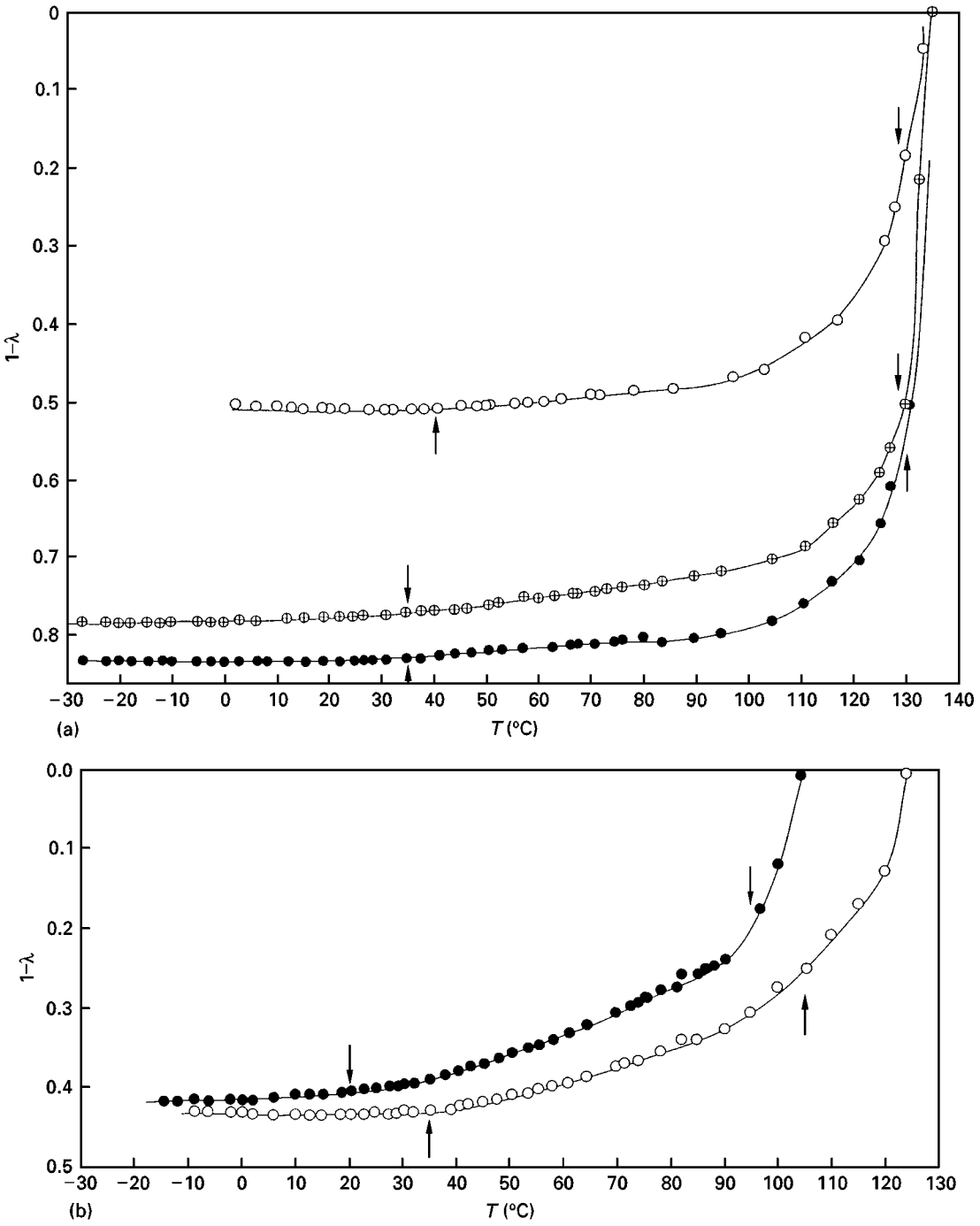

Figure 1 (a) Plot of crystallinity level, $1 - \lambda$, as determined from dilatometry, as a function of temperature for linear polyethylenes. (●), sample A, slowly cooled; (⊕), sample B, crystallized at 125 °C; (○), sample D, slowly cooled. For clarity, $1 - \lambda$ values are displaced by 0.02 and 0.06, respectively. Vertical arrows represent the onset of melting, T_i, and $T_{1/2}$ (Table II) the temperature at which the same is half melted. (b) Plot of the crystallinity level, $1 - \lambda$, as determined from dilatometry, as a function of temperature for branched polyethylene. (○), sample F; (●), sample G. The vertical arrows are the same as in (a).

sharper for the high-crystallinity sample, while the highest-molecular-weight polymers melt more broadly than the others. Indicated in Fig. 1 and also listed in Table II, are the temperatures, T_i, at which melting is first detected and the temperatures, $T_{1/2}$, that correspond to the disappearance of half of the initial crystallinity. Some of the changes that are observed in the tensile behaviour will be discussed in terms of the fusion process and the changing level of crystallinity. This is one of the few investigations where the tensile behaviour and course of fusion are studied concurrently on the same samples.

3.3. Yield stress

A plot of the yield stress against the deformation temperature is given in Fig. 2 for all the polymers studied here. The results can be placed into two distinct categories. Except for the lowest deformation temperature the linear polyethylenes (open symbols) fall into one group while the branched and copolymers (full symbols) are in another. At the lowest temperatures, the yield stresses of all the polymers are in the range 50–65 MPa. They are independent of the molecular constitution of the chains as well as the structural and morphological characteristics of the crystalline state. Brown and Ward [23] found very similar results for two linear polyethylenes whose molecular and structural characteristics were, however, similar to one another. The generalization can be made from the present results that in the low-temperature region (about $-100\,^{\circ}C$) the yield stress does not depend on either the molecular constitution of the chains or the structure and morphology in the crystalline state. This temperature region is close to or slightly above the glass temperature (γ transition) of both linear and branched polyethylenes [24–28]. Thus, as was suggested previously, the yield stresses of the glass and the crystalline region are close to one another [23].

When the deformation temperature exceeds the glass temperature region, the curves for the branched and linear polyethylenes clearly diverge from one another. The yield stresses of the linear polymers are greater and order according to the crystallinity level. The yield stress of the branched polymers decreases with increasing temperature at a rate that is approximately twice that of the linear polyethylene. Moreover, while the yield stress–temperature relation of each of the linear polyethylene samples delineate separate curves, the data for the three branched samples all fall on a common curve. However, at the highest deformation temperatures, $90\,^{\circ}C$ or above, the yield stresses of the linear polymers merge into one another.

Since the yield stresses of both linear and branched polyethylenes depend on the crystallinity level, particularly the core crystallinity [3–6], it is not surprising that the yield stresses of the branched polymers are lower than those of the linear polymers at temperatures above the glass temperature. Since the crystallinity levels of the three branched polymers are very close to one another (see Table II), we would also expect that their yield stresses would be similar, as is observed. The yield stresses of the branched polymers decrease smoothly and monotonically with increasing temperature. There is no indication of any discontinuity in the region of the β transition. Although this transition has been attributed to the glass temperature, it has, however, been shown to be a property of the interfacial region [29, 30]. The monotonic decrease in the yield stress over a wide temperature range is a reflection of the broad fusion range, and the attendant decrease in crystallinity. This type of melting is characteristic of random copolymers [31].

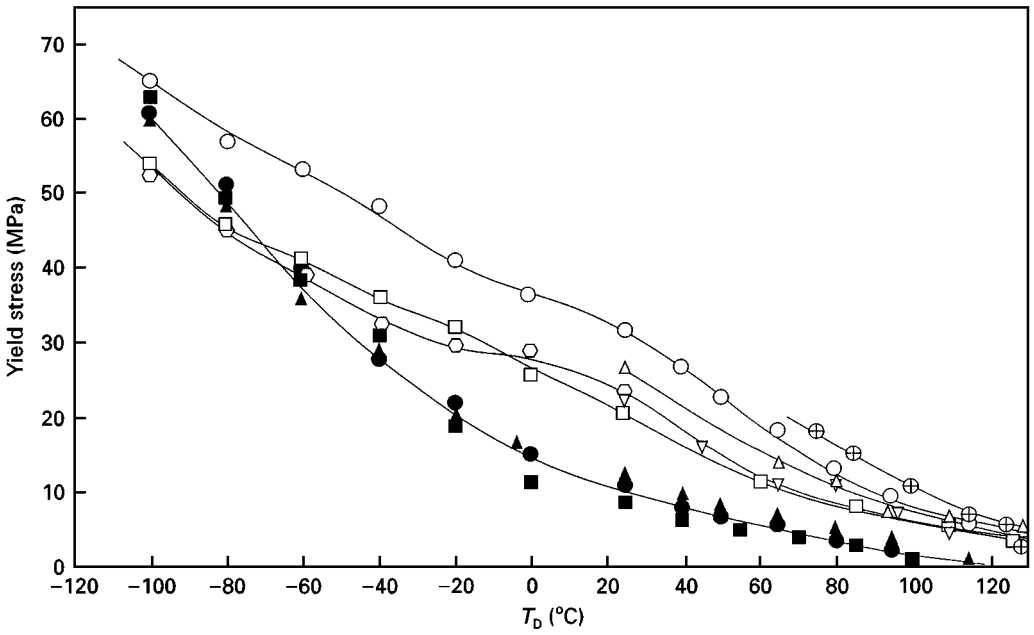

Figure 2 Plot of yield stress against deformation temperature for linear and branch polyethylenes. (○), sample A, slowly cooled; (⊕), sample A, crystallized at 128.5 °C; (□), sample B, quenched at −78 °C; (△), sample C, slowly cooled; (⬡) sample D, slowly cooled; sample E, slowly cooled; (●), sample F, slowly cooled; (■), sample G, quenched; (▲), sample H, slowly cooled.

The yield stress approaches zero in the vicinity of 100–115 °C. This temperature range is very close to the melting temperature. At slightly lower temperatures the yield stresses are very small, reflecting the very low levels of crystallinity.

The curves for the linear polyethylenes in Fig. 2 are quite different. From slightly above − 100 °C to about 90 °C each polymer delineates a separate curve. The separation between the curves is based on the crystallinity level. This dependence becomes very clear when the room-temperature yield stress is plotted against the crystallinity level. This correlation is well documented for a wide range of polyethylene samples covering a wide variety of structures and morphology [3, 6, 7, 32–35]. It is interesting to note that in the vicinity of 0 °C there is a change in slope in the yield stress–temperature curves. Above this temperature the decrease in yield stress becomes more rapid. The curves merge into one another at about 110 °C and appear to approach zero at temperatures slightly above 130 °C. The convergence close to the melting temperature has been observed by others [36–38]. This behaviour is a manifestation of the very low levels of crystallinity in the melting range for the linear polymers. The different temperature ranges between the linear and branched polymers for the approach to zero yield stress are due to the different melting temperatures, which in turn are due to the different chain structures. Similar results have been reported for the temperature at which the yield stress approaches zero [36–38].

Sample A, which was isothermally crystallized at 128.5 °C for 17 days, represents a special case. The crystallization conditions were chosen so as to achieve a very high degree of crystallinity, 0.90 on a density basis. At temperatures less than 75 °C the sample undergoes brittle failure and no yield maximum occurs prior to break. The onset of a ductile-type deformation at this temperature corresponds closely to the onset of melting, and a decrease in the crystallinity level, as determined by the dilatometric measurements. It has been shown that the ductile-to-brittle transition occurs sharply, with just small changes in the crystallinity level [5]. The result with this sample is consistent with the earlier observations.

It has been suggested that the yield stress is influenced by the location of the α transition [39]. The temperature, T_α, of the α transition depends primarily on the crystallite thickness, which can be varied systematically by changing the crystallization conditions [30]. To examine this postulate, sample B was crystallized under four different regimes that were so chosen that T_α should vary by about 40–50 °C [30]. The yield stress–temperature plots of four different specimens of polymer B, crystallized at different temperatures, are given in Fig. 3. The shapes of the curves in Fig. 3 are very similar to one another. The curves are displaced only according to their crystallinity levels. Therefore, we can conclude that the α transition plays a negligible role in the yielding process. We should also note that there is no correlation between the yield stress and the supermolecular structure as defined by small-angle light scattering.

The experimental findings with respect to the yield stress–temperature relations give some of the basic data necessary to examine some of the molecular and structural interpretations that have been suggested for yielding in semicrystalline polymers. Several different mechanisms have been proposed. One proposal is that yielding in crystalline polymers in general, and the polyethylenes in particular, involves the thermal activation of screw dislocations, with the Burgers vector being parallel to the polymer chain direction [40–43]. The expected dependence of the shear yield stress on the crystallite thickness and on the deformation temperature can be calculated from this dislocation

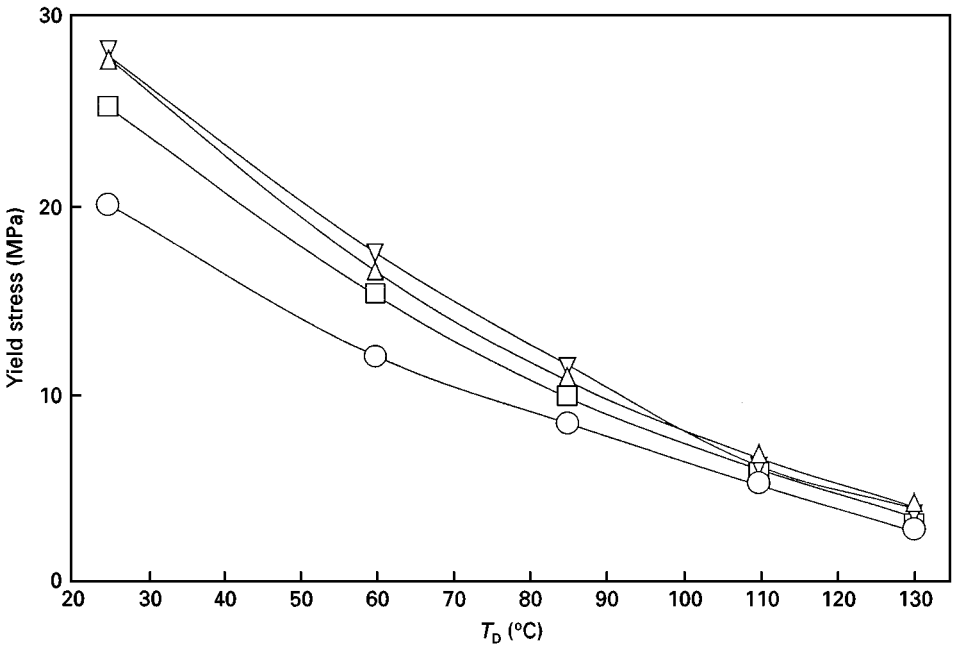

Figure 3 Plot of yield stress against deformation temperature for sample B crystallized under different conditions. (○), Quenched at − 78 °C; (□), crystallized at 90 °C for 30 min; (△), crystallized at 115 °C for 30 min; (▽), crystallized at 125 °C for 30 min.

model. An outline of the theory, sufficient for present purposes, is given below.

The free energy, ΔG, required to form a screw dislocation of Burgers vector, b, located at a distance, l, from the edge of crystallite of thickness, L_c, for a resolved shear stress, τ_y, is given by

$$\Delta G = \frac{kb^2 L_c}{2\pi} \ln\left(\frac{1}{r_0}\right) - blL_c\tau_y \tag{2}$$

Here k is a function of the shear modulus of the crystal, b is the magnitude of the Burgers vector, has the value of 25.4 nm, the c-axis dimension of the unit cell, and r is the core radius of the dislocation and is thought to be of the order of $2b$ [40–42]. The critical value of l that is required to activate the dislocation, designated as l_c, is obtained from the maximum in ΔG, ΔG_c. It is given by

$$l_c = \frac{kb}{2\pi\tau_y} \tag{3}$$

The corresponding activation energy for dislocation growth is given by

$$\Delta G_c = \frac{kb^2 L_c}{2\pi}\left[\ln\left(\frac{l_c}{r_0}\right) - 1\right] \tag{4}$$

From Equations 2 and 3, one obtains

$$\tau_y = \frac{k}{4\pi}\left[\exp\left(\frac{2\pi\Delta G_c}{kb^2 L_c} + 1\right)\right]^{-1} \tag{5}$$

Equation 5 directly relates the shear yield stress, τ_y, to the crystallite thickness, L_c, and to the temperature, through ΔG_c. ΔG_c is thought to be in the range of 30–80 kT [42].

Experimentally the tensile yield stress, σ_y, is measured. It can be converted to the required shear yield stress by the relation $\tau_y = \sigma_y/2$ [40–42]. Young [40–41] has suggested that the crystal, or reduced shear stress, defined as $\tau_y^0 \equiv \tau_y/\alpha_c$ be used. Crist et al. [42] however, used τ_y in analysing experimental data. It has been reported that Equation 5 did not hold for linear polyethylene, at a fixed deformation temperature, over a crystallite thickness range 1000–4000 nm, irrespective of whether the resolved yield stress, or "crystal" yield stress were used [6]. For random copolymers, when the thicknesses are usually restricted to the small range of 500–1000 nm a rationalization could be made for the dislocation theory in terms of the experimental results. On this basis, despite the lack of quantitative agreement between the theoretical expectations and the observed crystallite thickness the theory predicts the correct order of magnitude of the yield stress. The yield stress–temperature data given in Fig. 2 allow an assessment to be made of the validity of the temperature dependence as expressed by Equation 5.

In Fig. 4 a comparison is made between the expected temperature dependence of the resolved shear stress, as embodied in Equation (5), and some representative experimental results for both the linear and the branched polyethylenes. The theoretical plots given in the figure cover a range in parameters; ΔG_c from 30 kT to 80 kT and L_c from 1000 to 2000 nm. The experimental data selected for illustrative purposes are

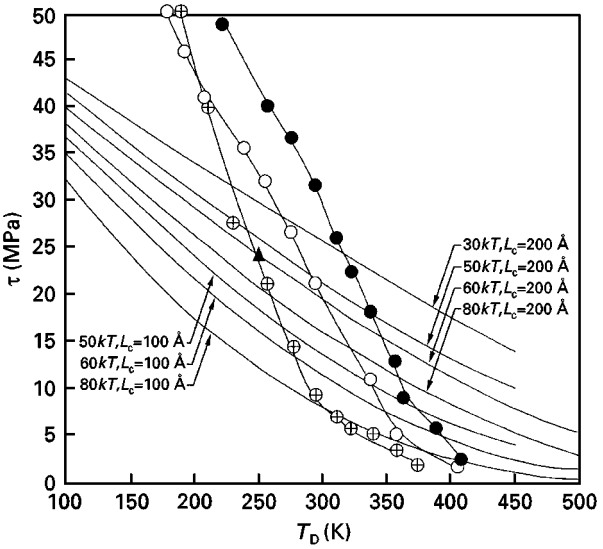

Figure 4 Plot of resolved shear stress τ against deformation temperature. Solid curves without data points, theoretical according to dislocation theory with values of ΔG^* and L_c indicated; solid curves through data points, experimental results (●), sample A, slowly cooled; (○), sample B, quenched at − 78 °C; (○), sample F, slowly cooled.

for slowly cooled sample A, quenched sample B and slowly cooled long-chain branched sample F. The other polymers studied follow a similar pattern. The shapes of all the theoretical curves are very similar to another. However, they are displaced from each other, depending on the values of ΔG_c and L_c. The shapes of the experimentally derived curves are also qualitatively similar to one another. The plots make clear, however, that the experimental curves are quite different from the theoretical expectation. The experimental curves are much steeper than the theoretical curves at low and moderate temperatures and actually intersect the theoretical curves at higher temperatures. This comparison is similar to the two examples cited by Crist *et al.* [42]. One can conclude that the dislocation theory, as it has been presented, does not satisfy the experimental data as far as the temperature dependence is concerned. However, as has been pointed out, the theory does predict the correct order of magnitude of the resolved shear stress at moderate temperatures.

It is well established that the yield stress is directly proportional to the core level of crystallinity. Thus, there are strong indications that changes in the structure of the crystallite, and the associated regions, are involved in the deformation process in the low-strain region. On the other hand, the shape of the force–length curve in the yield region is dependent on the molecular weight [3–6], crystallinity level [6] and the overall shape of the lamellar crystallites [44]. Thus, other factors, besides the crystallites themselves, must be involved in the yield process. It is apparent that the present form of the screw dislocation model needs to be modified.

In another approach to the problem, the deformation of highly oriented samples of linear polyethylene, which had single-crystal texture, was studied [45–48]. By design, therefore, only changes within the crystallite interior are studied. Consequently, only the

slippage of particular crystallographic planes were described and it was deduced that this process dominated over the complete deformation range.

In contrast with mechanisms restricted to changes within the crystallite interior, Flory and Yoon [49] have proposed that a partial melting–recrystallization process plays a major role in the total deformation. Under the applied stress, isothermal melting, abetted by any adiabatic heating of the smaller imperfect crystalline region will take place, followed by an oriented recrystallization. During the deformation, adiabatic heating will take place. However, a temperature rise is not required for the partial melting; the applied stress is adequate by itself. Therefore, the actual magnitude of any temperature rise is not directly pertinent to the proposed mechanism.

Small-angle neutron scattering studies of the deformation, in shear, of mixtures of deuterated and protonated linear polyethylene have demonstrated that, starting at elongations just beyond the yield point, partial melting–recrystallization is involved over the complete deformation range [50–52]. Similar scattering studies through the yield region have not as yet been reported. However, the investigations of Harrison and co-workers [53–56] and of Gent and co-workers [57, 58] supported the concept of the partial melting–crystallization mechanism during yielding. These latter studies pointed out that consideration needs to be given to other possible mechanisms for yielding, besides crystallographic type changes within the crystallite interior. In semicrystalline polymers, the stress must be transmitted through disordered, liquid-like and interfacial regions, as well as the ordered crystalline region. From the experimental results and theoretical implications, a unique mechanism cannot be assigned to the yielding process.

3.4. Draw ratio after break

The important ultimate property, the draw ratio λ_B, after break, is plotted against the deformation temperature in Fig. 5. Fig. 5a represents the data

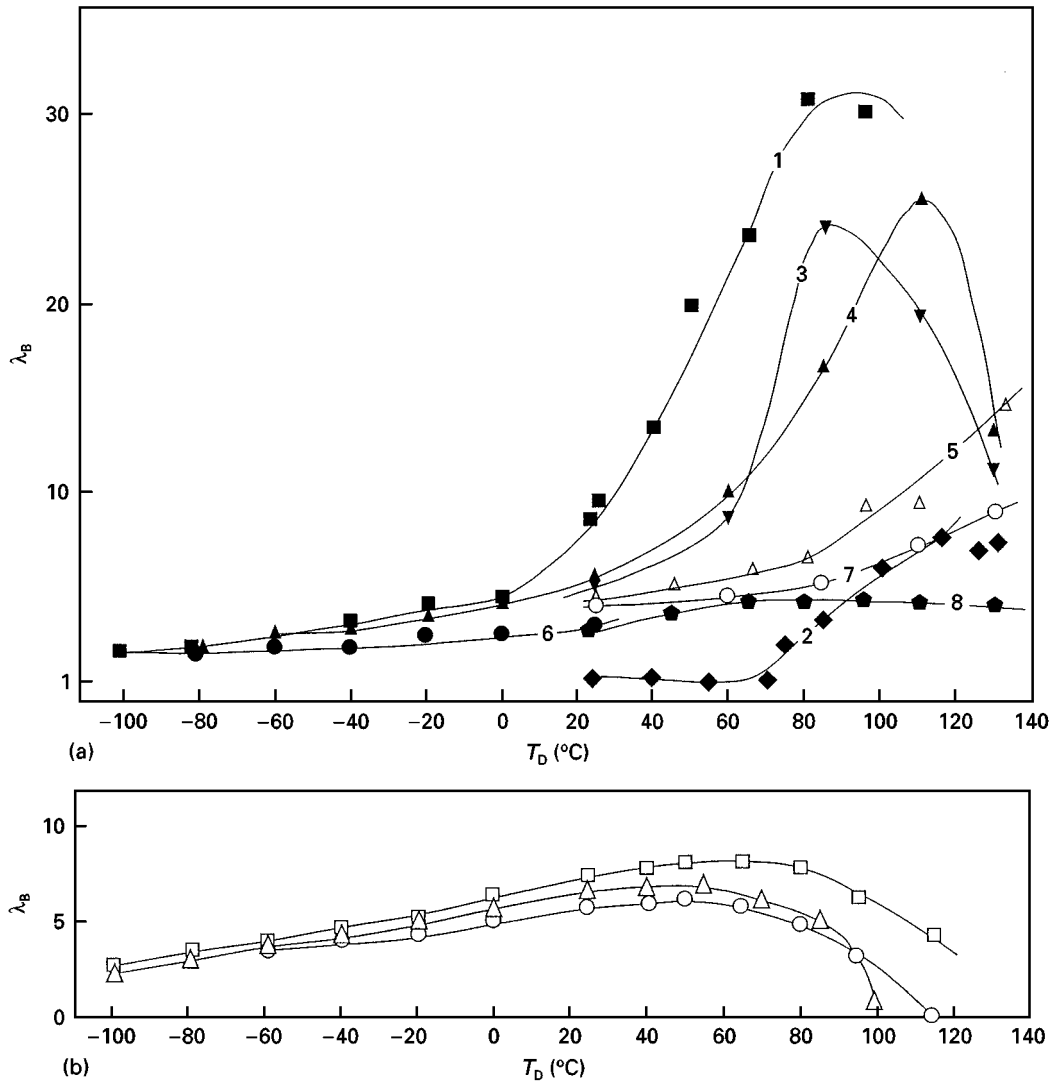

Figure 5 (a) Plot of draw ratio λ_B, after break, against deformation temperature for linear polyethylenes. (■), curve 1, sample A, slowly cooled; (◆), curve 2, sample A, crystallized at 128.5 °C for 17 days; (▼), curve 3, sample B, quenched at − 78 °C; (▲), curve 4, sample B, crystallized at 125 °C for 30 min; (△), curve 5, sample C, slowly cooled; (●), curve 6, sample D, slow cooled; (○), curve 7, sample D, crystallized at 120 °C for 30 min; (⬢) curve 8, sample E, slowly cooled. (b) Plot of draw ratio λ_B, after break, against deformation temperature for branched polyethylene. (○) sample F, slowly cooled; (△), sample G, quenched at − 78 °C; (□), sample H, slowly cooled.

for the homopolymers, while Fig. 5b shows those for the branched polymers. The curves for the branched polymers, all of which behave as copolymers from the point of view of crystallization behaviour, are quantitatively very similar to one another. These polymers show a slight, almost linear increase in λ_B up to a deformation temperature of about 30 °C. One of the main characteristics of these plots, a broad maximum in the range of about 30–80 °C, then appears. A sharp decrease in λ_B then follows as the melting temperatures are approached. The temperature interval of the broad maximum corresponds to the region where fusion is initiated and a significant amount of melting takes place (see Fig. 1b). The temperature range where the fusion process becomes accelerated, as the melting point is approached, corresponds to the decrease in λ_B with increasing temperature.

The temperature dependences of λ_B for the linear polyethylenes are quite different from those for the branched polymers. The highly crystalline specimen of sample A is brittle at temperatures below 75 °C and shows a unique behaviour (curve 2). All the other samples are ductile. The results for these samples fall into two main groups. At the lower deformation temperatures, the λ_B values of all the ductile samples are similar to one another and comparable with those of the branched polymers. Only slight increases are observed in λ_B up to temperatures of 20–40 °C. Starting in this temperature interval the behaviours of the ductile polymers begin to differ. This temperature range of 20–40 °C corresponds to the onset of melting as is observed dilatometrically. This temperature, defined as T_i, is indicated in Fig. 1 and is listed in the ninth column in Table II. Starting at about 20–30 °C, polymers having molecular weights equal to or less than 500 000 show a distinct rise in λ_B with temperature (curves 1,3 and 4). A maximum is reached for each sample in this group in the vicinity of 80–100 °C, depending on the polymer. A precipitous decrease in λ_B then occurs at the higher deformation temperatures. The temperature of the maximum in λ_B corresponds to the upsweep in the level of crystallinity with increasing temperature. The drop in λ_B corresponds to the temperature where about half the initial amount of crystallinity has melted. This temperature, also indicated in Fig. 1, is listed in the tenth column in Table II. Maxima have also been observed for molecular weights lower than those reported here [59]. There appears to be a tendency for the temperature that corresponds to the maximum to increase with increasing molecular weight. An effect of the strain rate on the location of the maximum has also been observed [59].

The temperature dependences of λ_B for the three highest-molecular-weight polymers studied, represented by curves e, g and h, are quite different from those of the lower-molecular-weight polymers. For these high molecular weights the pronounced upsweep in λ_B with increasing deformation temperature is no longer observed. Instead of rising to a maximum with increasing deformation temperature and then decreasing as the temperature is raised further, a rather broad plateau is observed in λ_B. Curve 5, representing Sample C ($M_w \simeq 1 \times 10^6$), is intermediate between the two extremes described. Starting at about 25 °C an increase in λ_B with increasing temperature is observed. This temperature corresponds to the onset of melting. A maximum is not reached at this strain rate up to a deformation temperature of 130 °C. However, the rate of increase in λ_B with the deformation temperature becomes greater with increasing temperature and portends to the distinct possibility that a maximum will be reached at a higher temperature.

The sample of polymer A that was isothermally crystallized to a degree of crystallinity of 0.90 on a density basis behaves quite differently from the others, as is illustrated by curve 50.8 mm Fig. 5a. This sample is brittle up to a deformation temperature of 75 °C. The draw ratio begins to increase above this temperature, indicating the onset of some element of ductility. This temperature corresponds to the initiation of melting as observed by dilatometry (see Table II). The fact that λ_B does not reach comparable values as the same polymer crystallized more rapidly to a lower crystallization level indicates that the deformation is still in the transition region.

Qualitatively similar relations between λ_B and the deformation temperature, for linear polyethylene samples having weight-averaged molecular weights less than 2×10^6 have been reported [38, 59, 60]. Capaccio *et al.* [61] only observed the upsweep portion of the curve in this molecular weight range, for deformation carried out at the faster draw rate of 101.6 mm min^{-1}. Jarecki and Meier [62] found qualitatively similar results for two linear polyethylenes in the lower molecular weight range at a draw rate of 50.8 mm min^{-1}.

The observed maximum requires the involvement of at least two mechanisms, each with a different temperature dependence. We have seen that for the lower molecular weights, where maxima are observed at the strain rate used here, a direct correlation can be made between the λ_B–temperature relation and the course of fusion. The fusion curves of the higher-molecular-weight samples are qualitatively very similar to those for the lower molecular weights, although the existence of maxima are only suggested. They are certainly not as distinct as are found in the lower-molecular-weight region. Therefore, the mechanisms involved have different molecular weight dependences and also depend on the strain rate.

A theoretical development directed to the understanding of the ultimate properties in a tensile-type deformation has been given by Termonia and Smith [63–66]. The model for the initially undeformed semicrystalline polymer is a network of entangled chains in random conformation. The presence of the crystallites is tacitly ignored in this theory. Two Eyring-type activated rate processes, each with its own set of constants, are assumed to govern the deformation. One of the postulated processes involved the breaking (but not re-forming) of the van der Waals interaction between the disordered chain units. The other process was assumed to involve slippage of chains through the entanglements. A simulation was thus carried out on an array of entanglements points, using Monte Carlo methods. Of particular interest to the problem at hand

is the predicted dependence of λ_B on the deformation temperature. Calculations, based on the theory, for molecular weight fractions show a very sharp essentially peaked, or spiked, maximum [63]. The temperature of the maximum depends on the strain rate. This expectation was confirmed by the results from one molecular weight fraction and a polydisperse sample [66]. It was stated that the maximum broadens as the polymer becomes more polydisperse. This conclusion is in qualitative accord with the observations reported here.

In an actual tensile deformation the initial isotropic semicrystalline system is transformed to an oriented fibrillar system. It is suggested, therefore, that a more realistic pair of mechanisms for the deformation past yield, each still following Eyring-type activated processed, can be postulated. On that follows the suggestion of Flory and Yoon [49] is that a partial melting–recrystallization process takes place. This mechanism would replace the breaking of van der Waals bonds. The other would be the deformation of the amorphous rubber-like region, with the entanglements serving as effective cross-links. Two Eyring-type processes would still be involved and the formalism of the theory could still be applied to the ultimate properties. Only the values of the parameter involved will change according to the specific processes assumed. The two mechanisms will obviously have different temperature coefficients and hence a maximum in λ_B will result. It would be expected that the contribution from the rubber-like deformation would be more molecular weight dependent since the entanglement density per chain would increase with increasing chain length. Hence the temperature of the maximum should increase with increasing molecular weight, at a constant strain rate, as is observed. The partial melting–recrystallization mechanism is consistent with the correlation that has been found between the course of fusion and the dependence of λ_B on the deformation temperature. It should not be as molecular weight dependent as the deformation of the non-crystalline region. The correlation that has been found here between λ_B, the deformation temperature and the course of fusion is important in understanding the processes that are involved.

The character of the curves in Fig. 5 make clear that it would be very misleading to draw any general conclusion regarding the overall deformation by limiting studies to only one molecular weight, or distribution, and one deformation temperature. It is clear that the process is very dependent on molecular weight and deformation temperature. Quite different results can be obtained as these variables are altered, at a constant strain rate, despite the fact that the crystallography, as represented by the unit cell, is the same in all the situations. A similar conclusion is reached when the strain rate is varied [59, 63]. Thus, a variety of factors are involved that need to be separated from each other.

Plots are given in Fig. 6 of λ_B against M_w for different deformation temperatures. At the lower molecular weights there is a relatively large change in λ_B with deformation temperature for a given polymer.

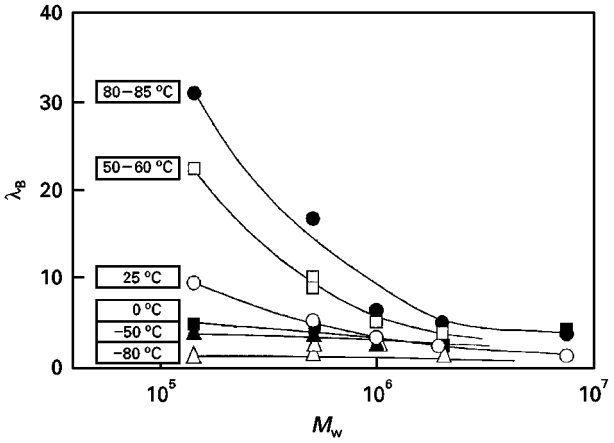

Figure 6 Plot of draw ratio, λ_B, against weight-averaged molecular weight, M_w, for indicated temperature for linear polyethylene.

For example, λ_B for the slowly cooled sample A ($M_w = 1.5 \times 10^5$) varies from a value of less than 2 at $-80\,^{\circ}C$ to 31 at $+80\,^{\circ}C$. At $25\,^{\circ}C$, λ_B is equal to about 10 for this polymer. The polymers in this range are undergoing a brittle-to-ductile transition as the temperature is raised. This transition has been shown to be very sensitive to the crystallinity level and occurs over only a small change in this quantity [5]. In contrast, the λ_B values of the ductile high-molecular-weight samples at high temperatures approach, or are very close to, the low-temperature values. In turn, the low-temperature values are invariant with molecular weight. In contrast with the lower molecular weight polymers, λ_B for sample C ($M_n = 2 \times 10^6$) only varies from 1.4 at $-80\,^{\circ}C$ to 6.6 at $80\,^{\circ}C$ and has a value of only about 3 at $25\,^{\circ}C$. This behaviour is clearly quite different from that of sample A. There are several different reasons why the high-molecular weight λ_B values are close to one another as a function of temperature. The fact that the λ_B values for all molecular weights are very close to one another at low temperatures is a consequence of the proximity of the deformation temperature to the glass temperature. The relatively low values of λ_B at the higher temperatures, for the ductile high-molecular-weight polymers, are due to the relatively high number of entanglements per chain. This in turn retards the deformation of the rubber-like region. In the ductile region, λ_B decreases with increasing M_w, as has been noted previously [3, 6].

3.5. Ultimate tensile strength

The TUTS, calculated in the manner that was described, is plotted as a function of temperature, in Fig. 7a and b for the linear and branched polymers respectively. The TUTS is remarkably constant for each of the linear polymers in the deformation temperature range from $-100\,^{\circ}C$ to $0\,^{\circ}C$. However, there is a significant difference in the stress levels between the polymers. Above $0\,^{\circ}C$, the trends in the TUTS are similar to those described in Fig. 5 for λ_B and can be categorized in a similar manner. This is not an unexpected result since the calculated TUTS is influenced

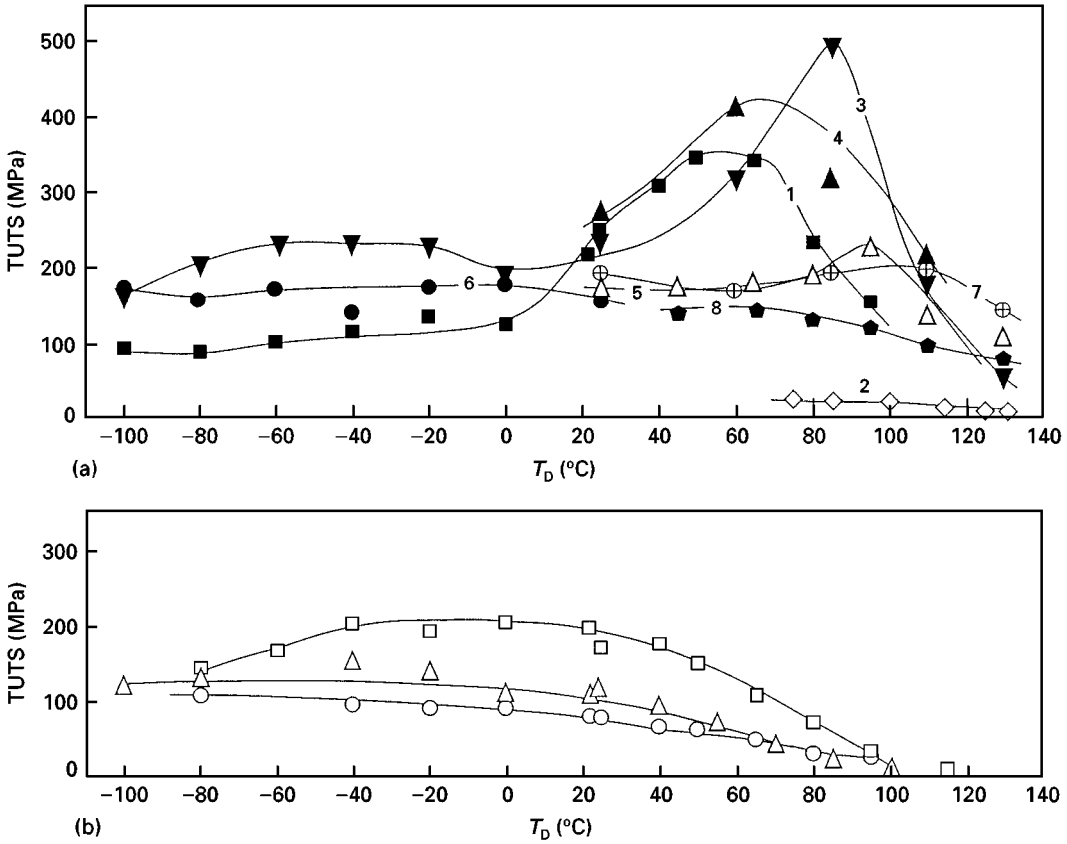

Figure 7 (a) Plot of TUTS against deformation temperature for linear polyethylenes. (■), curve 1, sample A, slowly cooled; (◇), curve 2, sample A, crystallized at 128.5 °C for 17 days; (▼), curve 3, sample B, quenched at − 78 °C; (▲), curve 4, sample B, crystallized at 125 °C for 30 min; (△), curve 5, sample C, slowly cooled; (●), curve 6, sample D, slowly cooled; (⊕), curve 7, sample D, crystallized at 120 °C for 30 min; (⬢) curve 8, sample E, slowly cooled. (b) Plot of TUTS against deformation temperature for branched polyethylene. (○) sample F, slowly cooled; (△), sample G, quenched; (□), sample H, slowly cooled.

by the ultimate cross-sectional area of the sample, which in turn decreases as λ_B increases.

In analogy to the results with λ_B (Fig. 5) a maximum is observed in Fig. 7a for the lowest-molecular-weight linear polymers in the ductile region. This molecular weight range is characterized by a modest number of entanglements per chain so that relatively large deformations can be attained, resulting in a high extent of chain orientation. At temperatures above the maximum, continuous partial melting and oriented recrystallization dominates, which in turn results in a decrease in the stress. The results for sample C ($M_w \simeq 1 \times 10^6$) (curve 5 in Fig. 7) only show a very weak maximum. The results for this molecular weight serve as a demarcation between the behaviour of the lower molecular weights and the very-high-molecular-weight linear polymers studied. If maxima exist for samples D and E, ($M_w = 2 \times 10^6$ and 8×10^6, respectively), they are barely perceptible. The high entanglement density per chain at these molecular weights retards the deformation of the non-crystalline portion of the system. The stress induced crystallization at the higher temperature causes a decrease in stress at the highest crystallization temperature. The gradual decrease in stress observed in Fig. 7b for the branched polymers, at deformation temperatures above 0 °C, can also be attributed to the domination of melting and stress-induced crystallization.

3.6. Force–elongation curves

The impression has been created that there is a unique force–elongation curve for semicrystalline polymers in general, and for the polyethylenes in particular [67, 68]. However, this concept has been dispelled by more recent work [3–6]. Since the yield stress and ultimate properties depend very strongly on molecular weight, the structural regularity of the chain and the deformation temperature, one would expect to observe a variety of force–length curves that have quite different characteristics. This expectation is indeed fulfilled. To examine these curves in a convenient and systematic manner we use the qualitative description of categories that was introduced previously for deformations carried out at room temperature [3].

Fig. 8 gives an example of the force–length curves, at different temperatures, for polymers that fall into category I at room temperature. At a deformation temperature of 0 °C, and below, the curves are characterized by a very sharp yield point, followed by a short plateau with increasing elongation and a limited range of strain hardening prior to break. This behaviour is consistent with the small values of λ_B that are observed at these low temperatures for polyethylenes in this class. No distinct neck is observed at the low deformation temperature. As the temperature is increased above 0 °C, the yield point is not quite as sharp and a diffuse neck develops. A much broader

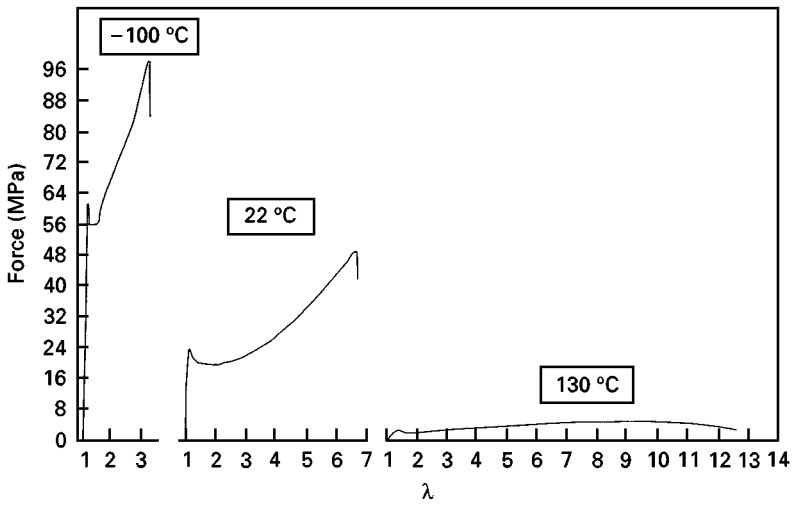

Figure 8 Plot of force against extension ratio, λ, for sample B quenched at − 78 °C at indicated deformation temperatures.

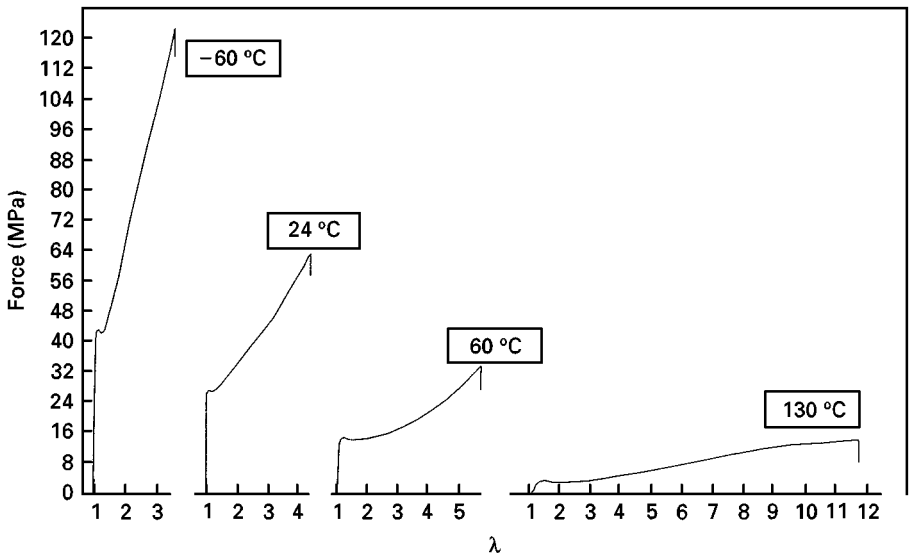

Figure 9 Plot of force against extension ratio, λ, for sample D crystallized at 120 °C for 30 min at indicated deformation temperatures.

strain-hardening region develops which results in a larger value of λ_B. At deformation temperatures greater than the maximum in λ_B, the neck, as observed visually, becomes less distinct. The strain-hardening region also becomes less well defined. Quite strikingly, the yield point becomes very diffuse. Similar changes have also been observed in force–elongation curves at room temperature with ethylene–α olefin copolymers as a function of increasing co-unit content and decreasing crystallinity level and for linear polyethylenes as the molecular weight increased [3, 6, 7].

A set of force–elongation curves for a high molecular weight sample is given in Fig. 9. The characteristics at room temperatures place this polymer in category III. The yield points, at room temperature and below, are not nearly as distinct as the results in Fig. 8 for a lower-molecular-weight sample. They become more diffuse with increasing deformation temperature as compared with the lower-molecular-weight sample of category I. The sharpness of the neck can be correlated with the sharpness of the yield point. Typical force–elongation curves for the highly crystalline $(1 - \lambda)_d = 0.90$ sample A is given in Fig. 10. At deformation temperatures of 75 °C and less the yield point is very sharp; brittle fracture occurs with λ_B slightly greater than 1. This behaviour is illustrated by the force–elongation curve at 75 °C. At higher temperatures, after some melting has ensued, the yield becomes more diffuse. The value of λ_B indicates that the deformation is in the transition region [5]. There is no indication of any strain hardening at the higher deformation temperatures.

Force–elongation curves for the ethylene–butene copolymer are given in Fig. 11 for different deformation temperatures. The general characteristics of these curves are similar to those of the high-molecular-weight linear polyethylene, shown in Fig. 9, particularly in the strain-hardening region. The depth of the yield point is, however, much greater than is found for the high-molecular- weight linear polymers. However, in contrast with linear polyethylenes of comparable molecular weight a distinct neck is visible at all

temperatures below ambient. The strain hardening–deformation temperature behaviour is comparable with that of linear polyethylenes of much higher molecular weights.

The enhanced strain hardening of high-molecular-weight linear polyethylene can be attributed to the large number of entanglements per chain and the resulting retardation of the rubber-like deformation. However, for one random-type copolymer, hydrogenated polybutadiene, it has been determined that the molecular weight between entanglements is greater than its linear counterpart [69]. Therefore, the deformation in the strain-hardening region for copolymers cannot be attributed to an enhanced modulus of the rubber-like regions. Another mechanism must be involved. A likely possibility is strain-induced crystallization. Such a process would enhance the strain hardening [70]. Therefore, there appear to be at least two possible structural bases for strain hardening. The contribution of each will be dependent on the structural characteristic of the chain.

4. Conclusions

The studies of the temperature dependence of tensile properties has enabled some general conclusions to be made with regard to the role of molecular constitution and the key structural parameters in the deformation process. The companion dilatometric studies have enabled a direct comparison to be made with the level of crystallinity and its changes with temperature.

At temperatures just above the glass temperature, the yield stresses of all the polymers are very close to one another, irrespective of whether they are linear or branched or their levels of crystallinity. At temperatures above the glass temperature, the yield stresses of the branched polymers delineate the same curve, reflecting the similarity in the crystallinity levels of these chains. On the other hand, in this temperature range the linear polyethylenes define separate curves that depend on the crystallinity level. The data for the linear polyethylenes converge at low levels of crystallinity for temperatures greater than 90 °C and become indistinguishable from one another as their respective melting temperatures are approached. These results indicate that the dominant structural factors at small deformations are the crystallite and associated regions. However, although the predicted order of magnitude is correct, the observed yield stress–temperature relations cannot be explained by the dislocation theory that has been developed to explain yielding.

At large deformations, there is a direct dependence on the molecular weight and the changing level of crystallinity. At least two competing mechanisms must be involved in this deformation region. The results can be qualitatively explained by postulating a partial melting–recrystallization process and a rubber-like deformation of the non-crystalline region. Strain-induced crystallization could also be involved. The extensive experimental results that have been presented can serve as a basis for a more quantitative theoretical development based on molecular and structural factors.

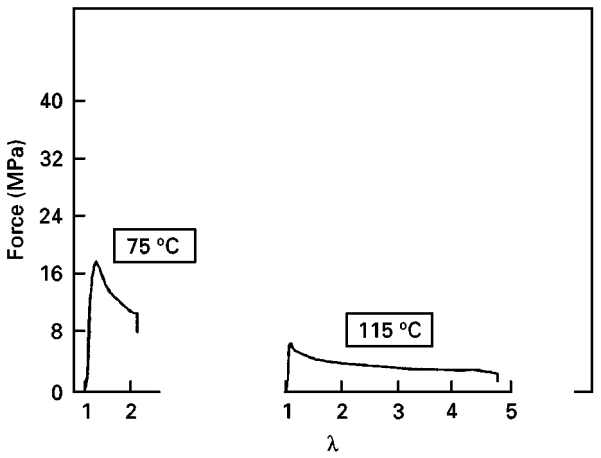

Figure 10 Plot of force against extension ratio, λ, for sample A crystallized at 128.5 °C for 17 days, at indicated deformation temperatures.

Acknowledgements

Support of this work by the National Science Foundation Polymer Program DMR 94-19508 is gratefully acknowledged. We wish to thank Dr C.S. Speed for carrying out the deformation measurements from − 100 °C to room temperatures.

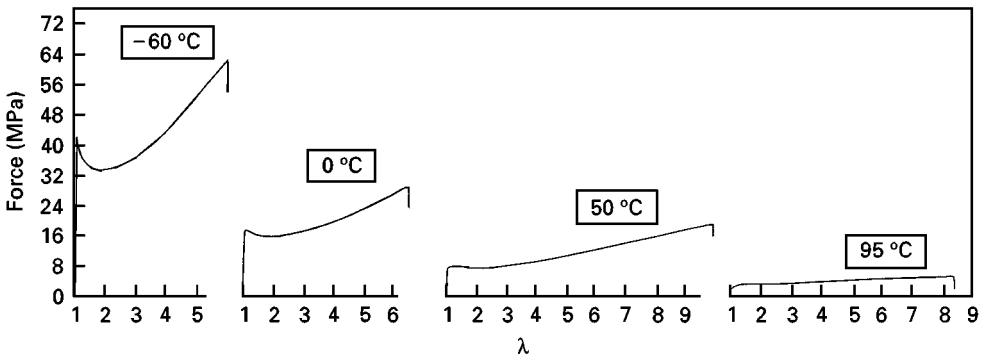

Figure 11 Plot of force against extension ratio, λ, for sample F slowly cooled, at indicated deformation temperatures.

References

1. L. MANDELKERN, *Polym. J.* **17** (1985) 337.
2. *Idem.*, *Accounts Chem. Res.* **23** (1990) 380.
3. R. POPLI and L. MANDELKERN, *J. Polym. Sci. Polym. Phys. Edn.* **25** (1987) 441.
4. A. J. PEACOCK and L. MANDELKERN, *ibid.* **28** (1990) 1917.
5. L. MANDELKERN, F. L. SMITH, M. FAILLA, M. A. KENNEDY and A. J. PEACOCK, *ibid.* **31** (1993) 491.
6. M. A. KENNEDY, A. J. PEACOCK and L. MANDELKERN, *Macromolecules* **27** (1994) 5297.
7. M. A. KENNEDY, A. J. PEACOCK, M. D. FAILLA, J. C. LUCAS and L. MANDELKERN, *ibid.* **28** (1995) 1407.
8. E. T. HSIEH and J. C. RANDALL, *ibid.* **15** (1982) 353.
9. *Idem.*, *ibid.* **15** (1982) 1402.
10. R. CHIANG and P. J. FLORY, *J. Amer. Chem. Soc.* **83** (1961) 2857.
11. F. A. QUINN, JR and L. MANDELKERN, *ibid.* **80** (1958) 3178.
12. G. R. STROBL and W. HAGEDORN, *J. Polym. Sci., Polym. Phys. Edn.* **16** (1978) 1181.
13. M. GLOTIN and L. MANDELKERN, *Colloid. Polym. Sci.* **260** (1982) 182.
14. L. MANDELKERN and A. J. PEACOCK, *Polym. Bull.* **16** (1986) 529.
15. M. FAILLA, R. G. ALAMO and L. MANDELKERN, *Polym. Testing* **11** (1992) 151.
16. J. MAXFIELD and L. MANDELKERN, *Macromolecules* **10** (1977) 1141.
17. L. MANDELKERN, *Discuss. Faraday Soc.* **68** (1979) 310.
18. N. BEKKEDAHL, *J. Res. Natl. Bur. Stand.* **43** (1949) 145.
19. C. H. BAKER and L. MANDELKERN, *Polymer* **7** (1966) 7.
20. E. ERGOZ, J. G. FATOU and L. MANDELKERN, *Macromolecules* **5** (1972) 147.
21. R. G. ALAMO and L. MANDELKERN, *ibid.* **24** (1991) 6480.
22. E. A. COLE and D. R. HOLMES, *J. Poly. Sci.* **46** (1960) 245.
23. N. BROWN and I. M. WARD, *J. Mater. Sci.* **18** (1983) 405.
24. F. C. STEHLING, E. ERGOZ and L. MANDELKERN, *Macromolecules* **4** (1971) 672.
25. C. L. BEATTY and F. E. KARASZ, *J. Macromol. Sci. Rev. Macromol. Chem. C* **17** (1971) 37.
26. J. SIMON, C. L. BEATTY and F.E. KARASZ, *J. Therm. Anal.* **7** (1975) 187.
27. A. H. WILLBOURN, *Trans. Faraday Soc.* **54** (1958) 717.
28. E. W. FISCHER and F. KLOOS, *J. Polym. Sci., Polym. Lett. B* **8** (1970) 685.
29. R. POPLI and L. MANDELKERN, *Polym. Bull.* **9** (1983) 260.
30. R. POPLI, M. GLOTIN, L. MANDELKERN and R.S. BENSON, *J. Polym. Sci., Polym. Phys. Edn.* **22** (1984) 407.
31. P. J. FLORY, *Trans. Faraday Soc.* **51** (1955) 848.
32. C. A. SPERATI, W. A. FRANTA and H. W. STARKWEATHER, *J. Amer. Chem. Soc.* **75** (1953) 6127.
33. G. R. WILLIAMSON, B. WRIGHT and R. W. HAWARD, *J. Appl. Chem.* **14** (1964) 131.
34. A. TRAINOR, R. N. HAWARD and J. N. HAY, *J. Polym. Sci., Polym. Phys. Edn.* **15** (1977) 1077.
35. P. B. BOWDEN and R. J. YOUNG, *J. Mater. Sci.* **9** (1974) 2034.
36. B. HARTMANN, G. F. LEE and R. F. COLE, *Polym. Engng. Sci.* **26** (1986) 554.
37. R. SEGUELA and F. RIETSCH, *Polymer* **27** (1986) 703.
38. A. N. KARASEV, I. N. ANHEYEVA, N. M. DOMAYENA, K. I. KOSMATYKLI, M. G. KARASEVA and N.A. DOMMICHEVA, *Vysokomol. Soyed. A* **12** (1970) 1127.
39. R. W. TRUSS, P. L. CLARKE, R. A. DUCKETT and I.M. WARD, *J. Polym. Sci., Polym. Phys. Edn.* **22** (1984) 191.
40. R. J. YOUNG, *Mater. Forum* **11** (1988) 210.
41. *Idem.*, *Phil. Mag.* **30** (1974) 85.
42. B. CRIST, C.J. FISCHER and P.R. HOWARD, *Macromolecules* **22** (1989) 1709.
43. B. CRIST, *Polym. Commun.* **30** (1989) 69.
44. J. T. GRAHAM, R. G. ALAMO and L. MANDELKERN, *J. Polym. Sci. B, Polym. Phys.* **35** (1997) 213.
45. L. LIN and A. S. ARGON, *J. Mater. Sci.* **29** (1994) 294.
46. A. GALESKI, Z. BARTEZAK, A. S. ARGON and R. E. COHEN, *Macromolecules* **25** (1992) 5705.
47. Z. BARTCZAK, A. S. ARGON and R. E. COHEN, *ibid.* **22** (1992) 5036.
48. *Idem.*, *Polymer* **35** (1996) 3427.
49. P. J. FLORY and D. Y. YOON, *Nature* **272** (1978) 226.
50. G. W. WIGNALL and W. WU, *Polym. Commun.* **24** (1983) 334.
51. W. WU, G. D. WIGNALL and L. MANDELKERN, *Polymer* **33** (1992) 4137.
52. B. K. ANNIS, J. STRIZAK, G. D. WIGNALL, R. G. ALAMO and L. MANDELKERN, *ibid.* **37** (1996) 137.
53. T. JUSKA and I. R. HARRISON, *Polym. Engng. Rev.* **2** (1982) 14.
54. T. M. LIU, T. D. JUSKA and I. R. HARRISON, *Polymer* **27** (1985) 247.
55. T. LIU, I. R. HARRISON, *Polymer* **28** (1987) 1861.
56. *Idem.*, *Polym. Engng. Sci.* **27** (1987) 1399.
57. A. N. GENT and J. JEONG, *ibid.* **26** (1986) 285.
58. A. N. GENT and S. MADAN, *J. Polym. Sci. B, Polym. Phys.* **27** (1989) 1529.
59. F. L. SMITH and L. MANDELKERN, to be published.
60. R. CORNELUSSEN and A. PETERLIN, *Makromol. Chem.* **105** (1967) 193.
61. G. CAPACCIO, T.A. CROMPTON and I. M. WARD, *J. Polym. Sci.: Polym. Phys. Edn.* **18** (1980) 301.
62. L. JARECKI and D. J. MEIER, *Polymer* **20** (1979) 1078.
63. Y. TERMONIA and P. SMITH, *Macromolecules* **20** (1987) 835.
64. *Idem.*, *ibid. Macromolecules* **21** (1988) 3485.
65. *Idem.*, *ibid. Macromolecules* **21** (1988) 2184.
66. *Idem.*, *ibid. Colloid. Polym. Sci.* **270** (1992) 1085.
67. J. H. MAGILL "Treatise on materials science and technology", edited by J. M. Schultz (Academic Press, New York, 1977).
68. B. WUNDERLICH, "Macromolecular physics" (Academic Press, New York, 1973).
69. J. M. CARELLA, W. W. GRAESSLEY and L. J. FETTERS, *Macromolecules* **17** (1984) 2275.
70. P. J. FLORY, "Principle of polymer chemistry" (Cornell Press, Ithaca, NY, 1953).

Received 3 November 1997
and accepted 5 February 1998